

Modelling of the lava flow of the Holocene eruption of El Lentiscal, Gran Canaria

Ismael

Lemes

Samper

Curso

2021/2022

**Nombre
tutor/es:
Alejandro
Rodríguez
González**

Trabajo Fin de Título para la obtención del título en Ciencias del Mar

Abstract-----	3
1.- Introduction -----	3
1.1.- Geographic Information Systems-----	5
1.2.- Location and Holocene volcanism of the island of Gran Canaria: case of the El Lentiscal eruption.-----	7
2.- Volcanic morphology: Paleo-morphological and topographical reconstruction. ----	10
2.1.- Topographical reconstruction. -----	10
2.2.- Morphological reconstruction-----	15
3.- Petrological and geochemical description of the eruption of El Lentiscal -----	17
3.1.- Petrography -----	17
3.2.- Geochemical-----	18
4.- Lava flow modelling-----	18
5.- Q-LavHA and its integration into simulation models-----	21
6.- Analysis of the El Lentiscal eruption simulation. -----	23
6.1.- Importance of the parameters used. -----	23
6.2.- Constraints on lava length and their implication for simulation models. -----	27
6.3.- DEM characteristics and their implications for simulations -----	30
7.- Conclusion -----	32
8.- Discussion-----	33
Appendix -----	34
Bibliography -----	36

Abstract

Volcanic eruptions are very destructive events that change the lives of humans in a short period of time. The island of Gran Canaria, as it belongs to a Volcanic archipelago, is not exempted from this danger. This work focuses on a small Holocene eruption in the municipality of Santa Brígida, which is known as the El Lentiscal eruption. From the work carried out with the QGIS program, the terrain has been topographically reconstructed, as well as obtaining morphological data. A series of simulations have also been carried out with the Q-LavHA plugin, the main objective of this work is to understand the behavior of the lava flow on the ground.

1.- Introduction

Volcanic eruptions are natural events with a huge destructive power. This turns volcanic buildings into true engulfers of cities and claims hundreds of humans' lives. Despite this, the human species has had to live with these events throughout its history. All volcanic episodes have influenced both positively and negatively the lives of humans. The case of the Canary Islands is no exception, in fact we are an archipelago made up entirely of volcanic materials. Due to the proximity in which the population are established to some volcanoes, there is a high danger in terms of life, health and belongings of the people who settle in these areas. A clear example is the eruption of the Cumbre Vieja volcano in La Palma, which left entire towns like Todoque buried under lava. In addition, the closer we get to the source of the emission, the danger increases.

The high population density of these areas is due to high fertility, despite the high danger they entail. Some examples that can be provided of developed cities in the vicinity of high volcanic hazard areas could be the city of Naples on the slopes of Mount Vesuvius (one of the most active volcanoes in Europe) (figure 1.1A and B) and the city of Auckland in New Zealand (the volcanically active region with the highest population density in the world) (figure 1.1 C and D). These areas, having a high porosity, which is a characteristic of volcanic regions, are loaded with nutrients, making them very useful soils, but highly dangerous.



Figure 1.1.- Examples of cities that have developed in volcanic areas: A) City of Naples with Mount Vesuvius in the background, B) Satellite view of Mount Vesuvius (*Google Earth*, 2022), C) City of Auckland with Mount Eden in the middle of the city, D) Satellite view of Auckland (*Google Earth*, 2022).

Today, knowing the geological processes behind each volcano plays an important role to protect people. Thus, it is proposed to carry out research on volcanism from Geographic Information Systems (GIS) in order to obtain necessary information and understand the behaviour of future eruptions. This research can be a powerful tool that allows us to combine different types of results such as topography, rock chronology and composition, morphology, etc. These results are inserted into a database to study the evolution of the volcano in the space and time. With all this, the information is contained in thematic maps, which reflect all the necessary information such as the virulence of the eruption, the range of action and the possible distribution of the lava in the region. All these results that can be obtained are a fundamental tool for the security forces since they provide them with knowledge on how to manage a volcanic alert and prepare emergency plans.

This thesis focuses on the study of lava flows, choosing the most dangerous ones, since, according to the records, they are the most common in Gran Canaria. The hazard associated with lava flows are fire and burial. However, there are many occasions in

which attempts have been made to divert the flow with different methods (barriers, diversion channels, cooling the lava with water jets, etc) but most cases have ended in failure.

Over the years, modelling and simulation of volcanic events have been developed, which has allowed us to have a better understanding of possible future eruptions, thus knowing the possible areas affected by the lava flow, where they appear and when. These questions can be answered with greater certainty with the generation of volcanic hazard maps from detailed investigations of past eruption together with the prediction of the simulation models that have been developed.

This paper focused on the numerical simulation of the lava flows of El Lentiscal, based on a series of parameters collected in previous studies that characterize the eruption. Nevertheless, the challenge proposed by the numerical simulations is the optimization of the software to reduce the execution times of these simulations, which gives us the best approximation to reality. As quite a few simulation models have been developed over the years, both deterministic models (focus their attention on the physicochemical parameters of the eruption) and probabilistic models (topography plays an important role in controlling lava flows), will be used to compare the results by applying the Q-LavHA application. This tool runs under an open-source software called QGIS.

Finally, it will be possible to evaluate the possible effects of an eruption anywhere in the world. All this can be applied thanks to the GIS methodology used in this paper in the eruption of El Lentiscal.

1.1.- Geographic Information Systems

Nowadays, Geographic Information Systems have generated a rapid conceptual and practical evolution for the management and analysis of geographic information and represent a breakthrough in the conception of maps as a form of geographic expression of the terrain. It is a relatively young new field of technology that incorporates graphical features with which we can evaluate real-world problems (Rodríguez González, 2009).

Before moving on to the study of aspects related to GIS, several important issues need to be addressed. First, the data that is introduced into a GIS handles geometric and topological information of the geographic units, which marks a series of different practices that generate practical problems and differentiate it from other information systems. Moreover, the geographic information is very voluminous unlike the

information that we can handle with conventional databases, therefore the complexity will depend on the resolution considered (Rodríguez González, 2009).

In itself, geographic information is very ambiguous: how can we know where a river bank is located between a river and its estuary? We can say that geographic information is multiform depending on the needs proposed by the user. The key is to be found in the word "Geography", this implies that all data is spatial, i.e. they are linked in certain ways to locators on the ground. In addition, we can add additional information associated to the spatial data such as attributes (Rodríguez González, 2009).

A GIS uses several levels (Figure 1.2). At the most basic levels it can be used as a mapping tool. Nevertheless, the real potential of this tool lies in using different spatial and statistical methods in order to analyze attributes and geographic information (Rodríguez González, 2009). The information generated can be divided into derived information, interpolated information or priority information (Antenucci *et al.*, 1991).

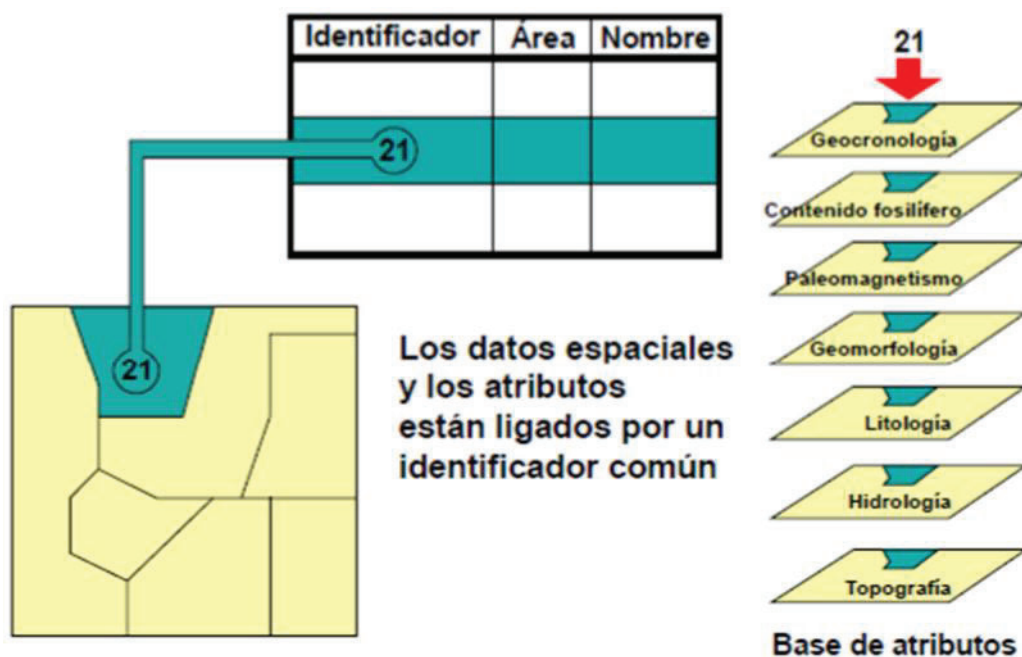


Figure 1.2: Levels of a GIS (Rodríguez González, 2009).

The GIS discipline is relatively young with a certain complexity and immaturity with some issues to be resolved. Though, like all disciplines, it contains a theoretical framework already established with conceptual issues and its own methodology well differentiated from the rest of the disciplines (Rodríguez González, 2009).

GIS are included within the scope of information systems (IS), which are defined as technological tools to respond to problems that are not solved beforehand. These IS included databases, knowledge bases and a user interaction interface. We will not only refer to IS as computational processes. For this reason, the term "computer-based systems" (CBS) is more frequently used nowadays. By using this term, we are stating that IS are more than just their own characteristics: they also have a decision-making tendency (Rodríguez González, 2009).

Therefore, GIS does not have only one definition. Over the years, attempts have been made to establish several definitions. Some authors emphasize GIS as databases (Dueker, 1979; Goodchild, 1985; SMITH et al., 1987), other authors define GIS by their functionalities (Clarke, 1986; Masser, 2014; Raveneau, 1988) and others like Cowen, 1988 defined them by their importance in decision support systems. But all these definitions have a specific central point which is the fact of working with data that are georeferenced. Currently, when talking about GIS, the general thinking is that of computerized systems (Rodríguez González, 2009).

As a final point, nowadays we can find in the market a huge amount of GIS software, either commercial or open source. Some of this software are TNTmips (MicroImages), ArcGIS (ESRI), ArcView (ESRI), QGIS, etc. For this paper we have used QGIS software because it is an open source and easy to use.

1.2.- Location and Holocene volcanism of the island of Gran Canaria: case of the El Lentiscal eruption.

We are located in the Canary archipelago to the NW of the African coast. It is part of a group of archipelago known as the Macaronesian formed by Azores, Madeira, Canary Islands and Cape Verde located to the NE of the Atlantic Ocean between latitudes 14°-40° N (subtropical situation) and bordering the coast of Africa. This archipelago is made up of seven islands (Lanzarote, Fuerteventura, Gran Canaria, Tenerife, La Gomera, La Palma and El Hierro), four islets (Lobos Island to the N of Fuerteventura, and La Graciosa, Montaña Clara and Alegranza to the N of Lanzarote) and numerous rocks.

Gran Canaria, the island where our study area is located, occupies a central position in the archipelago. Morphologically speaking we are facing a cupuliform building, with an almost circular base of about 45 km in diameter and a transverse profile crowned by the Pico de las Nieves with a height of 1950 m. It is an island deeply scarped by a network

of ravines that flow radially from the summit to the coastal sectors, thus generating a very abrupt orography with significant slopes. The coastline of the island is quite irregular, with very vertical cliffs in the western sector of the island contrasting with the wide platforms and beaches of the eastern and southern coastal sectors.

Holocene volcanism on the island of Gran Canaria is concentrated in the northern part of the island. A total of 34 emission centers have been identified and mapped, including main cones, parasitic cones, hornitos and fissures (Figure 1.3). This volcanism is characterized by small Strombolian volcanoes with open horseshoe craters conditioned by changes in slope, the type of relief from which the emission centers arise and the predominance of trade winds. Also, the presence of phreatomagmatic calderas that have left traces kilometers away from the emission center can be highlighted (Rodríguez González, 2009).

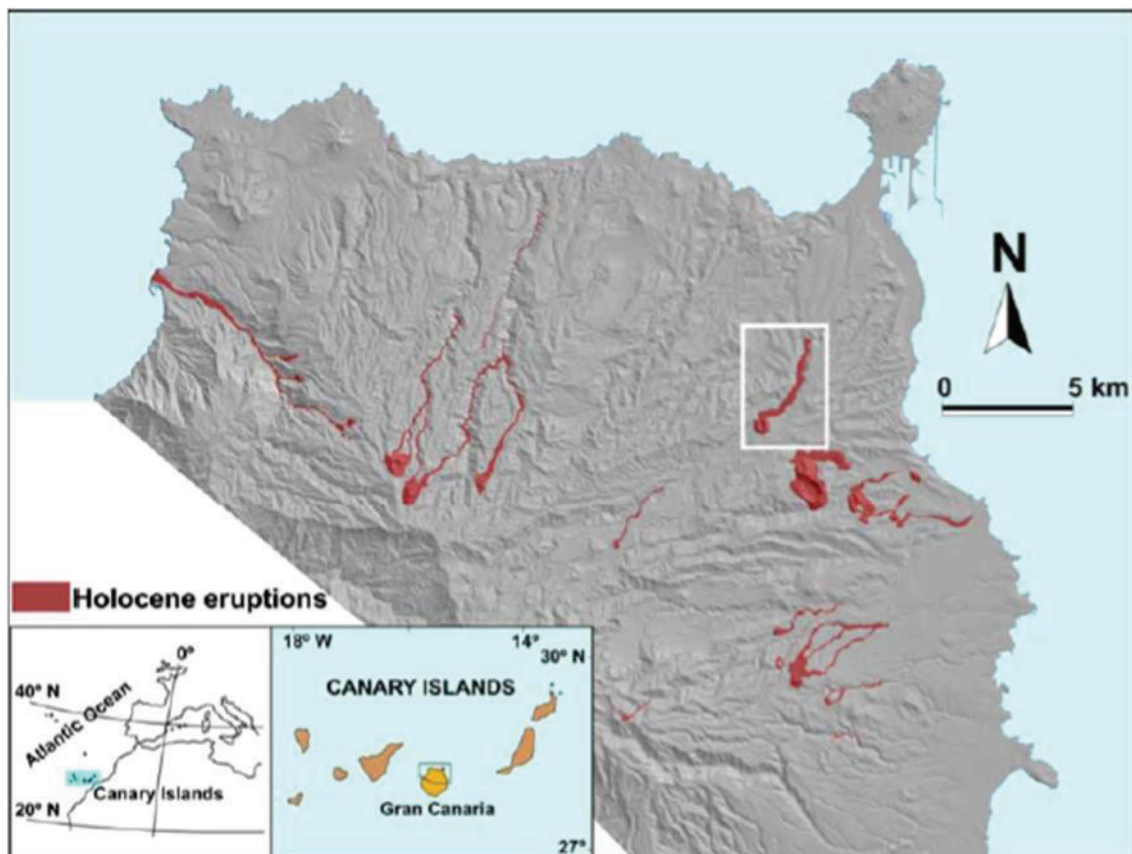


Figure 1.3: Location of the 34 emission centers recorded in the Holocene in Gran Canaria, our study area (El Lentiscal) is marked (Rodríguez-Gonzalez et al., 2010).

The study area is in the municipality of Santa Brígida. The volcanic edifice grows on a divide known as Coello mountain that intercepts the Guinguada ravine.

The eruption of El Lentiscal left an open cone in a horseshoe shape and towards the north in favor of the slope. The volcanic cone presents a scoriaceous internal structure, with strata very inclined towards the interior and with a smooth surface (Figure 1.4). However, the strata present on the outer flanks of the building is inclined in favor of the slope, with those on the slope being steeper than those on the divide or at the bottom of the ravine (Rodríguez González, 2009).

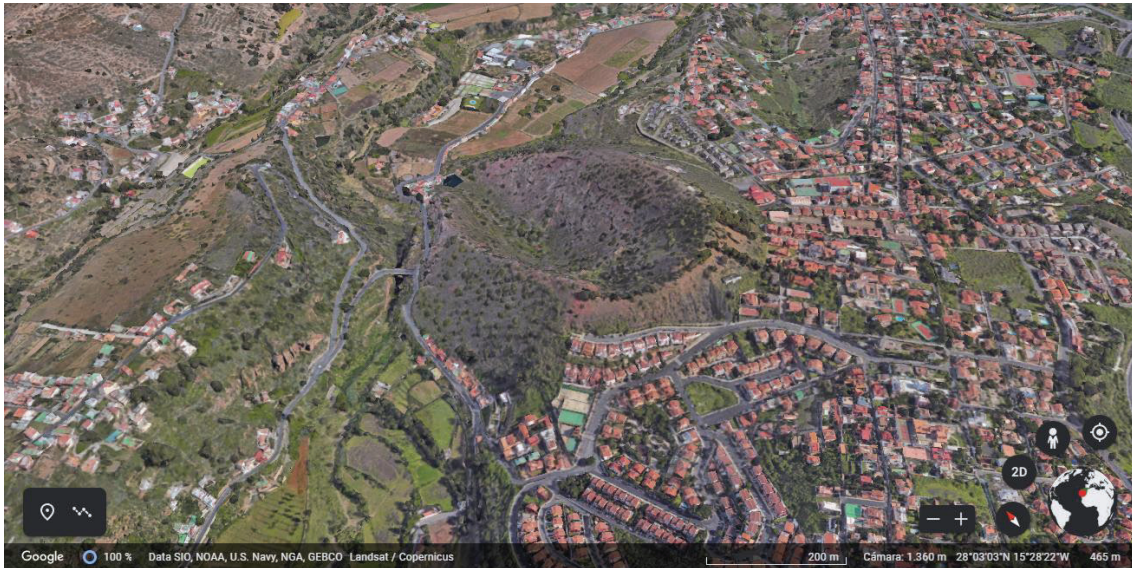


Figure 1.4: Aerial view of the volcanic edifice of El Lentiscal (*Google Earth*, 2022).

The lava flow emerges from inside the crater and is channeled directly into the Guinguada ravine. Along the lava surface we can find erratic blocks up to 10 m high (Figure 1.5). Morphologically speaking, the lava flow has a scoriaceous structure at the top, being more massive towards the interior. The effects of erosion affect the lateral axes of the lava flow, mainly affecting the more scoriaceous, less compact areas (Rodríguez González, 2009).



Figure 1.5: Erratic block on the lava flow of the El Lentiscal eruption.

2.- Volcanic morphology: Paleo-morphological and topographical reconstruction.

All volcanoes have a common morphology, presenting a main cone, the lava flow and the mantle of dispersing pyroclasts. All these structures are known as volcanic units and can be easily distinguished in the field. For the description of the units, we analyze the morphological aspects, which is our main contribution of data on how the current volcanic edifice could have originated. In this section of the study we will know how the terrain has evolved up to our days, our main way of study, using the GIS software.

2.1.- Topographical reconstruction.

A topographic reconstruction is understood as the return of a certain elevation of the terrain to obtain a possible pre-eruption situation. Firstly, after the field investigations, important data can be obtained to recognize and identify the volcanic units of our study area. For this purpose, GIS software will be used to describe the El Lentiscal eruption. However, the study of the lava flow will be our main avenue of study.

The first step for the topographic reconstruction of the study area is to make a geological map where the volcanic units are differentiated: volcanic cone, lava flow and mantle of horizontally dispersed pyroclasts (Figure 2.1). The dispersion of the pyroclasts is south of the cone formation due to the influence of the trade winds. Likewise, the lava flow is in NE direction of the cone, which as we have provided in section 1.2 presents numerous erratic blocks on its surface (see figure 1.5) (Rodríguez-

Gonzalez et al., 2018). To achieve such results, a vector layer characterizing each of the mentioned units on a DEM (Digital Elevation Model) and from field observations is available digitized. In addition, a dismantling by the action of external geological agents is predicted by studying an eruption with an age of approximately 2450 ± 60 years (Rodriguez-Gonzalez et al., 2010).

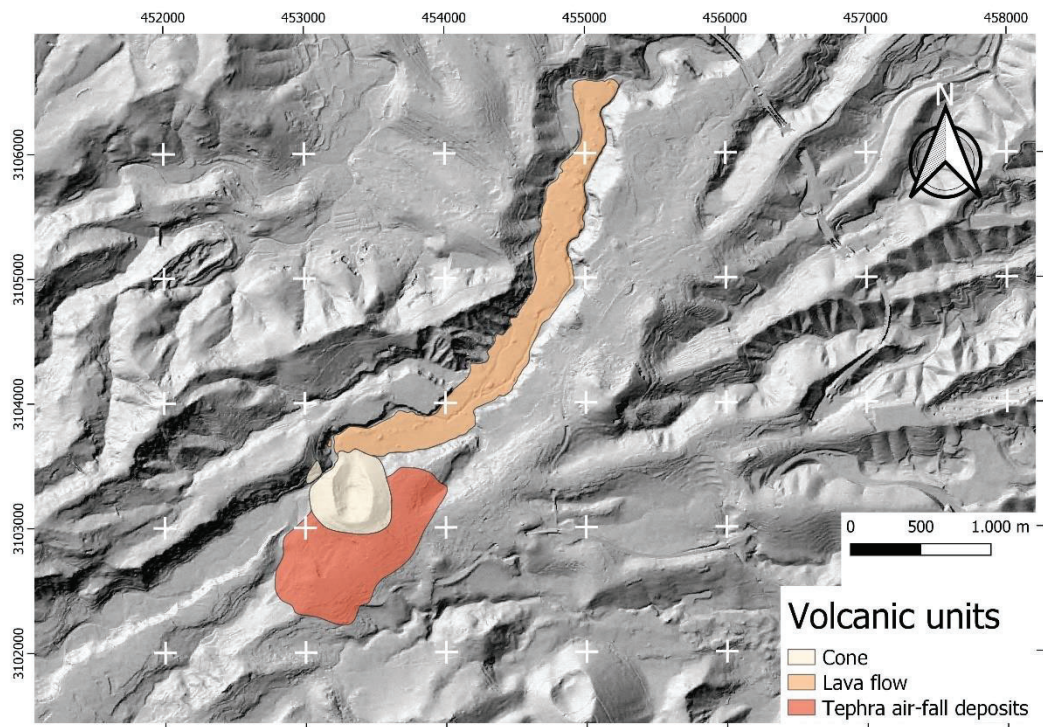


Figure 2.1: Geologic map of the El Lentiscal eruption.

The lava flow and the cone are digitized units that provide us with data on their respective surfaces. Moreover, when combined with the DEM raster of the study area we can obtain other data such as terrain elevation, slopes or crater depth as we can see in table 2.1, where all the morphometric data of the eruption of Mount Lentiscal have been compiled. All the data provided in the table are fundamental to know in detail the topography. They are also data that we will use later to develop modeling such as lava flow simulation.

Table 2.1: Morphometric data of the cone of eruption El Lentiscal.

Volcanic cone	Units	El Lentiscal data
Crater rim maximum elevation	m	500
Crater rim major axis (acr)	m	536
Crater rim minor axis (bcr)	m	285
Crater rim eccentricity (ecr)		0.8

Crater major axis azimuth (theta)	degrees	352
Crater depth (hcr)	m	130
Cone major axis (aco)	m	715
Cone minor axis (bco)	m	604
Cone eccentricity (eco)		0.5
Cone major axis azimuth (theta)	degrees	335
Cone height (h)	m	123
Cone volume (V)	m ³	10601500
Area (A)	m ²	344817
Cone slope (beta)	degrees	
Median	degrees	
Mean	degrees	26
Minimum	degrees	2
Maximum	degrees	52
Standard deviation	degrees	10
Basement slope (pre-eruption)	degrees	
Median	degrees	
Mean	degrees	15
Minimum	degrees	1
Maximum	degrees	59
Standard deviation	degrees	9

The lava flow is studied from different profiles perpendicular to the longitudinal displacement of the lava itself, which is a line that is digitized on the polygon of the lava flow. This analysis that we have performed gives us data on the length of the lava flow, the width of the flow channel and other data such as the elevation at each point of that length, in this case we have made 38 profiles. From all these data obtained in the analysis, we will obtain different parameters to facilitate their implementation in the following sections (Table 2.2).

Table 2.2: Morphometric data of lava flow of eruption El Lentiscal.

Lava flow	Units	El Lentiscal
Length (L)	m	3975
Bottom width (wb)		
Median	m	265
Mean	m	260
Minimum	m	134
Maximum	m	351
Standard deviation	m	54
Area (A)	m ²	994448
Height (h) (thickness)	m	

Median	m	13
Mean	m	13
Minimum	m	4
Maximum	m	24
Standard deviation	m	5
Volume (V)	m ³	9936530
Lava flow basis		
slope		
	degree	
Median	s	4
	degree	
Mean	s	3
	degree	
Minimum	s	0
	degree	
Maximum	s	9
	degree	
Standard deviation	s	3

With all the morphometric data collected so far, it is possible to reconstruct the entire area affected by the eruption, modifying the existing contour lines manually through GIS software. The contour lines are consciously modified, knowing that the relief prior to the eruption was much more uniform in the absence of the volcanic units. Topographic reconstructions are not usually performed at once, because several field observations are needed to understand and interpret the contour lines. The first step in the reconstruction is to remove the actual volcanic units of the El Lentiscal eruption and then modify the contour lines to obtain a more uniform surface. In addition, the holes generated by the erosion of the ravine can be filled by comparing the pre- and post-eruptive situations. Also, there is the possibility of obtaining the relief with the lava flow intact without the incision of the Guinguada ravine.

It should be noted that the same results can be obtained from current digital maps or with maps of historical records. However, the latter method is much more laborious because it must be scanned, georeferenced, vectorized and finally modified contour lines.

Once the topography is modified, topographic maps (vector) can be transformed to DEMs (raster) and the latter to digital shadow models. As can be seen in Figure 2.2 and 2.3, the changes that occur in the relief prior to the eruption are easily distinguishable,

highlighting the elevation of the volcanic cone on the divide and the filling of the bottom of the ravine.

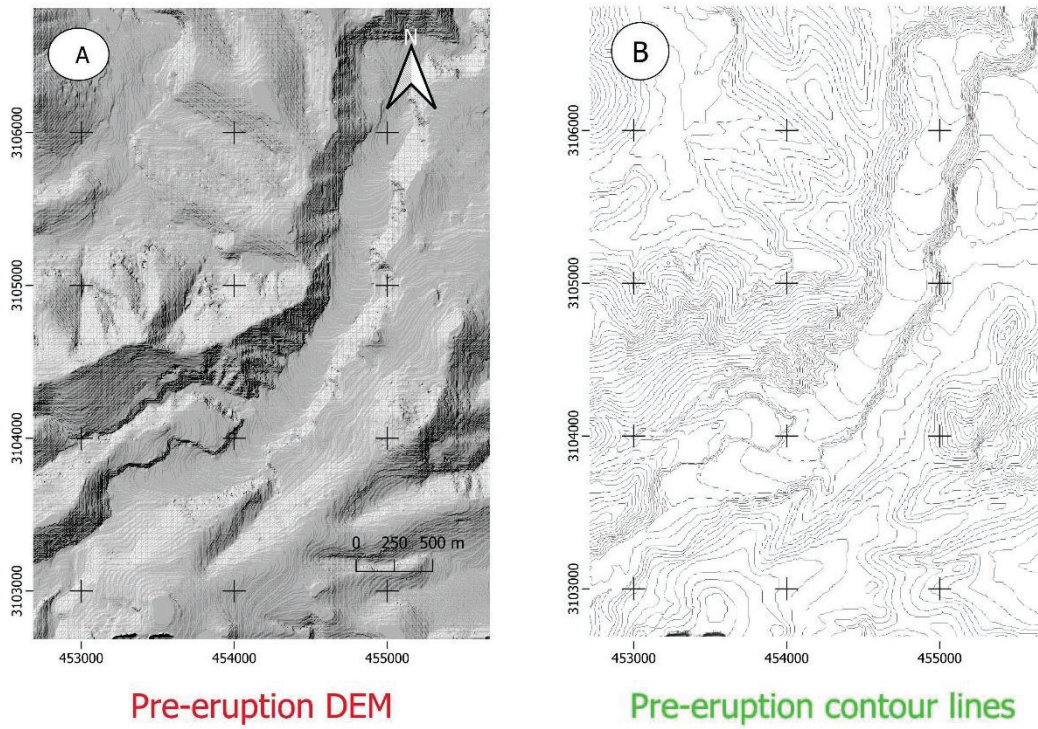


Figure 2.2: A) A shadow map of pre-eruptive relief. B) Contour lines before the eruption.

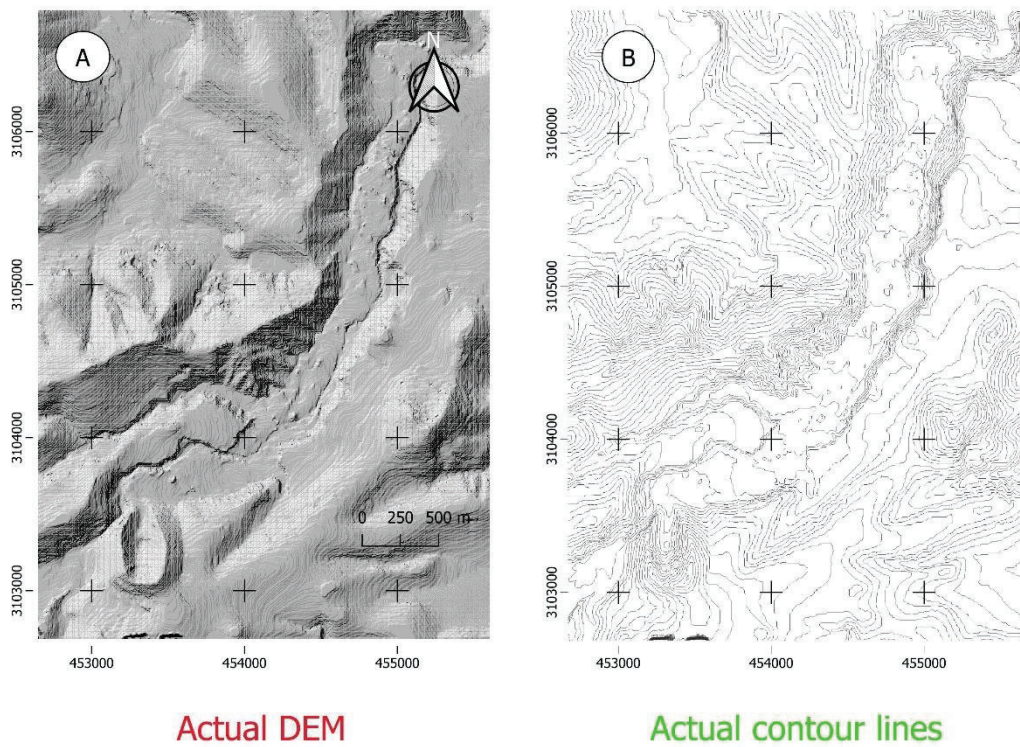


Figure 2.3: A) Actual DEM of the eruption of El Lentiscal. B) Actual contour lines of El Lentiscal.

2.2.- Morphological reconstruction

The geomorphological reconstruction data do not provide the necessary information on the evolution of the relief after the eruption. Like all eruptions, the eruption of El Lentiscal began with the opening of a fissure on the surface. The magma that emerges makes its way through the areas with little resistance and the weakest areas. This fact makes the emission center of our study eruption originated in a slope of the paleo-barranco del Guinguada. The lava flowed from the crater to the bottom of the ravine and advanced along the channel filling it until it stopped at about 3975 m from the emission center. Figure 2.4 shows three profiles at different times of the eruption (pre-eruption, post-eruption and current state). The pre-eruptive state (Figure 2.4 A) shows a U-shaped paleo-barranco with gently sloping hillsides. In the post-eruptive state (Figure 2.4 B), lava invades the bottom of the gully creating a plug preventing the passage of water transported by the gully. Finally, the current state (Figure 2.4 C), shows how the action of external geological agents (in our case the Guinguada ravine channel) has affected the lava flow.

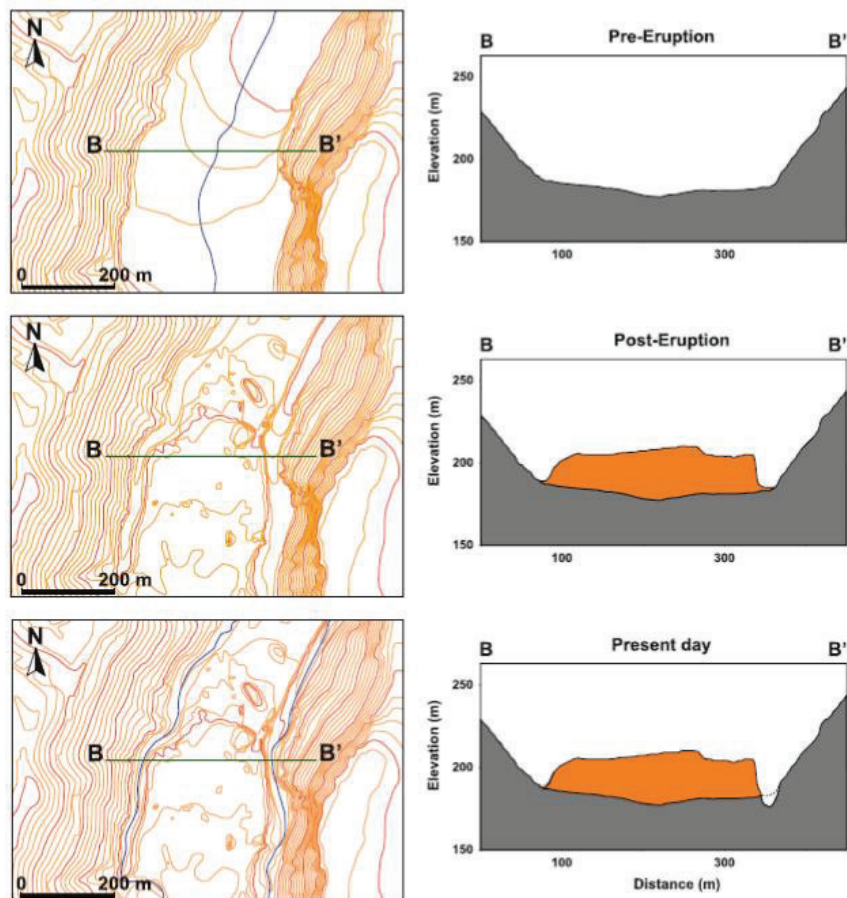


Figure 2.4: Geomorphological reconstruction of the lava flow of the El Lentiscal eruption (Rodríguez-González et al., 2010).

The same work that has been done with the lava flow is done with the formation of the volcanic cone. Figure 2.5 shows three profiles of the three eruptive moments. The pre-eruptive situation (Figure 2.5 A), shows a profile with no cone on the slope of the gully. Then, in the post-eruptive situation (Figure 2.5 B), the volcanic cone invades the paleogully generating a water plug in the gully. Currently (Figure 2.5 C), the northern slope of the cone has been dismantled after the passage of the Guinguada gully.

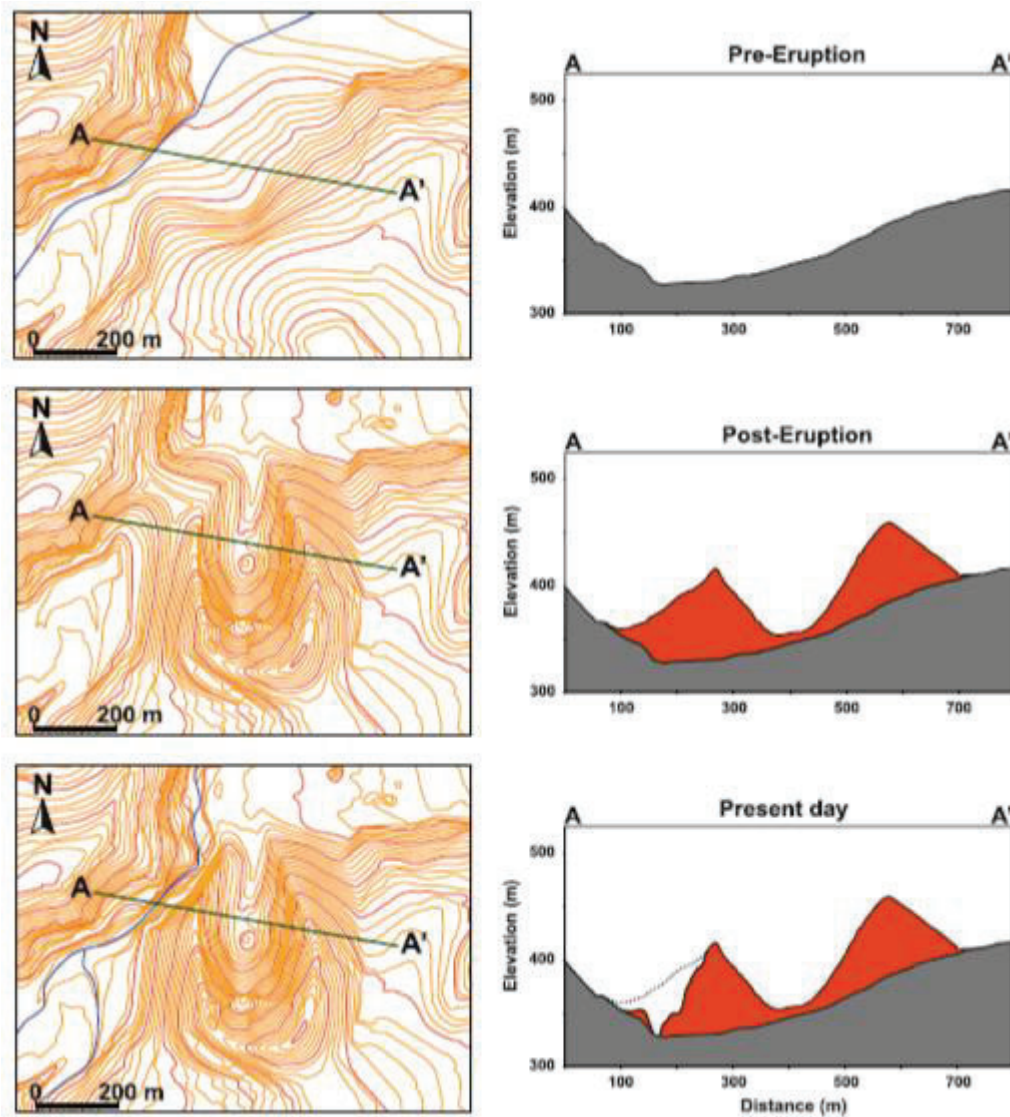


Figure 2.5: Cone profiles at different times during eruption (Rodríguez-Gonzalez et al., 2010).

After reconstruction from maps and profiles, the evolution of the terrain over the field can be understood. As can be seen in Figure 2.6, a reconstruction of both the cone and the lava flow can be performed.

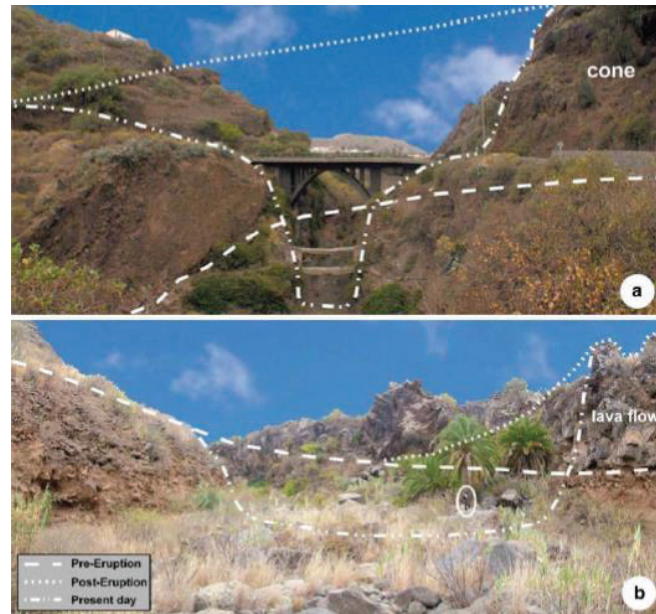


Figure 2.6: Details of the morphological reconstruction in the field of the cone (a) and lava flow (b) of the El Lentiscal eruption (Rodríguez-Gonzalez et al., 2010).

Once we have finished with the morphological reconstruction, a cut and fill analysis can be performed using our GIS software to obtain volumetric data for all volcanic units. The total volume (V_0) can be obtained with the overlapping of the pre-eruption and current eruption results. At the same time, with the difference of the current and pre-eruption surfaces we can calculate the actual volume of the ejected materials in the eruption (V_A). Therefore, the volume of dislodged material (V_D) is the difference between the total volume and the actual volume of the retained materials (Rodríguez González, 2009).

3.- Petrological and geochemical description of the eruption of El Lentiscal

3.1.- Petrography

In general, all Holocene lava flows from Gran Canaria have the same petrographic characteristics. All these lavas show a main aphanitic and porphyritic texture. In addition, another very common texture found is the vesicular texture. Other textures such as glomeroporphyritic and microlitic are also found (Rodríguez González, 2009).

Studying in detail the lava flow of the El Lentiscal eruption, according to the study carried out by Rodríguez González, 2009, this lava contains an inequigranular, porphyritic and vesicular texture. Also noteworthy is the greater amount of olivine compared to clinopyroxene. In addition, other crystals that can be found are plagioclase and opaque (Rodríguez González, 2009).

the greater presence of olivine provides information about the high fractionation that was generated in the magmatic chamber, allowing the formation of those green crystals characteristic of olivine.

3.2.- Geochemical

Geochemical analyses reveal that the Holocene lavas of Gran Canaria are very fresh and homogeneous, both from the textural point of view, because most of them belong to the alkaline series and the great majority are within the compositional range of the tephrites-basanites, and from the mineralogical point of view. This suggests that fractional crystallization processes and magma mixing are not dominant.

According to studies carried out by Rodriguez Gonzales, 2009, the Silica content of the lava from the El Lentiscal eruption is 43.42% and a $\text{Na}_2\text{O}+\text{K}_2\text{O}$ content of 5.46. With these data it can be observed that the lava belongs to the alkaline series due to its low Si_2O content, being a type of basanitic lava.

4.- Lava flow modelling

Some important aspects to consider are the type of lava composition, the nature of the lava and the territory through which it flows. Another aspect to consider being the one that is of more interest in our work is the behavior of the lava flow or its way of flowing in the natural environment. Related to our work, the degree of danger of the eruption is inversely proportional to the size of the material expelled by the eruption. In other words, if the materials flow silently out of the emitting source, lava will flow through the ground.

Lava is a type of non-Newtonian fluid known as Bingham. This is because the dynamic functioning of the fluid is based on the cohesion of the elements belonging to the magma and also to gravity, which allows it to move down the slope. Therefore, the lava spreads along the sides with a tendency to equilibrate in height and width, which means that it spreads out in width until it reaches a certain length. This event is totally independent of the terrain through which the lava flows. In addition, there are so-called lava boundary conditions. This imposes certain limits where the shear stress is not sufficient to allow the lava to advance. So, if the only limit is the floor, there will be no movement due to friction. This also occurs on the sides, forming the characteristic lateral lips or "levees" (Riello, 2002).

As long as the lava emission center continues to expel material, the lava flow continues to advance along the territory through which it flows. This is because the new material pushes the material at the lava front, resulting in the total advance of lava. Once the lava emission ceases, the lava flow reaches a state of equilibrium where it begins to cool and crystallize.

Analyzing the motion of a lava flow is a rather complex process due to the great majority of characteristics that define its nature. Also the numerical modeling is not far behind in terms of complexity since it is necessary to discretize certain parameters of a Bingham fluid that describe it. In addition, it must be understood that the motion is generated from a viscous thrust influenced by gravity. All these factors are the ones we will have to introduce in the algorithm. On the other hand, the determination of certain parameters governing the equations requires laboratory experimentation and the exploration of certain resources.

The difficulty involved in this type of studies has led to the creation of different numerical simulation methods to better understand the movement of lava. For this purpose, they have been classified into two main models:

- **Deterministic models:** This type of models are based on the discretization of the transport theory from differential equations that describe the conservation of mass, momentum and energy advance. The resulting equations (Navier-Stokes equations) are not linear and, since they do not have boundary conditions, free surface information and energy losses, obtaining results is complicated. Therefore, several approaches are applied to the Bingham fluid theory. The modeling is most simplified by simplifying the equations describing the motion. In our work we have chosen to use the model provided by the Q-LavHA plugin, the FLOWGO model of Harris & Rowland (2001). There are other models that have been proposed over the years such as, for example, FLOWFRONT by Young & Wudge (1990) or LavaSIM by Hidaka et al. (2005).

FLOWGO: It is a self-adaptive numerical model for a lava flowing inside a channel. The basis of this model is based on the estimation of the lava velocity as a Bingham fluid inside a channel. Throughout the simulation, heat losses and heat gains are calculated to determine the rheology of the lava (fluid dynamics).

The simulation will stop when the flow reaches the solid state or when the velocity is 0. This model requires a series of physicochemical parameters (Appendix I) and was validated in different volcanoes such as Mauna Loa in Hawaii or Mount Etna in Italy (Harris & Rowland, 2001).

- **Probabilistic models:** This type of model is based on the fact that topography is the main factor controlling the advance of the lava flow. Therefore, this model is able to identify areas potentially invaded by lava and calculate the probability that a DEM pixel will be flooded. It takes into account the impossibility that a pixel with a greater height than another is impossible to fill. Unlike deterministic models, this type of model is not computationally intensive. As in the case of the deterministic models, we again chose to use the two models provided by Q-LavHA:

Maximum length (L_{max}): Defines a maximum length (m) up to which the lava can flow, understood as the distance that the flow line travels and not the total distance of the lava flow. This distance can be obtained by studying the historical eruptions of the volcano we are studying (Mossoux et al., 2016). The length data we enter in the software must be multiplied by an empirically tested factor (Appendix II).

Decreasing probability: assumes that the probability that the lava flow reaches a certain length can be expressed with a decreasing cumulative density equation, following a normal distribution. Then, the probability of pixel flooding is weighted by the mean and standard deviation of the length of the historical eruptions of a volcano or of the same period (Appendix III), as we performed in this work, reviewing the Holocene period of Gran Canaria (Mossoux et al., 2016).

Although in this study we have used the models, they are not the only ones that exist. Currently, new models have emerged to improve the investigations with respect to volcanic hazard. The first one, MrLavaLoba (de' Michieli Vitturi & Tarquini, 2018), its operation is based on a probabilistic law of the steepest slope direction. That is, the computational processes try to guess which pixels are more likely to be flooded by the lava flow and the thickness it can reach. It is very similar to the L_{max} model mentioned

above, but with the possibility of applying it to pahoehoe lavas. The second place, we have the MULTIFLOW model (Richardson & Karlstrom, 2019), this model aims to go beyond a single flow line as there are interactions between the route and the topography where the lava flows. The topography, many times, being very irregular gives rise to possible branching of the "main" flow. Therefore, the algorithm quantifies the most important topography lengths that can influence the flow path. In addition, this model includes a threshold function that limits the extent of the lava flow according to the thickness it can reach.

5.- Q-LavHA and its integration into simulation models

Q-LavHA is a free plugin created to work in an open-source cross-platform geographic information systems environment distributed by the QGIS website. Once installed, it is incorporated in the QGIS add-on bar, through which we can access the plugin (Mossoux et al., 2016). Such plugin aims at simulating a flow by calculating the probability of flooding pixels through one or several emission points regularly distributed over a DEM with an iterative approach. Depending on the options defined by us, this plug-in calculates a series of predefined flow lines (in an iterative way) which is combined with the simulation parameters activated to express the probability of a pixel being flooded with lava.

Moreover, this add-on has the capability of combining probabilistic models with deterministic models and proposing improved calculations for the probability of lava flow propagation and the final length (Mossoux et al., 2016). This function allows users to evaluate, compare and finally choose the most appropriate model for our work, based on the available data and knowledge of the lava flows to be modeled.

Once we are in the Q-LavHA interface, it presents 4 sections. All these sections have the purpose of entering parameters. These parameters can be saved during the simulation process or introduced during the previous ones:

1. **"Vent location"**: In this section all parameters about the geographical location are entered. Here you choose the DEM to be used for the simulation, the type of lava emission source and insert the coordinates of the emission source.
2. **"Lava Flow Parameter"**: In this section you enter data about lava flow characteristics such as heights or length. Here you enter the minimum and average thickness values, and enable or disable "H16" or "Probability to the

square". H16 is used for DEMs analysis at 16 pixels, while Probability to the square gives the possibility for the flow lines to take the steepest slope path. In addition, the simulation model to be used is chosen in this section. These options differ from each other depending on the model used: Maximum length (Lmax) needs only one parameter; Decreasing Probability needs two and FLOWGO needs several physicochemical parameters as we saw in the previous section.

3. **"Output file"**: In this section the information about the generated output file is provided. In it, the vector layer of the current lava contour must be entered to calculate the fitness index (FI) of the simulation.
4. **"Advance setting"**: In this section, sensitivity tests can be performed for some specific input parameters.

Once the simulation is run, the code starts running. The equations that each model uses are extracted directly from the DEM, by elevating the pixels surrounding the flow. According to the models, one or several pixels (maximum 8) surrounding the point where the lava can propagate are selected. For this purpose, the slope is taken into account, since, as explained in the previous section, lava behaves as a Bingham flow and its flow goes in favor of the slope. Therefore, the probability of a pixel being flooded is directly proportional to the slope. In the case that it is negative (upward slope) the flow simulation stops because the probability is 0. However, if the next pixel is at a much lower level and constitutes a depression such as to be overcome by the correction factors that have been set, Q-LavHA expands its scan to 16 surrounding pixels of the lava flow (Figure 5.1A). If one of these 16 pixels does not meet the set requirements, the lava flow simulation stops its propagation.

To determine whether a pixel is flooded or not, the altitude at which the pixel surface is located is taken into account. This check is simple to understand: if the difference between the elevation at which the lava is located and the next one is positive, the pixel can be flooded and continue its propagation, being able to pass possible topographic obstacles. To make this possible, some correction factors are introduced, taking into account the values of the minimum lava thickness (H_c) and the average (H_p). The latter allows overpassing deeper depressions that can generate an erroneous stopping of the simulation (Figure 5.1B).

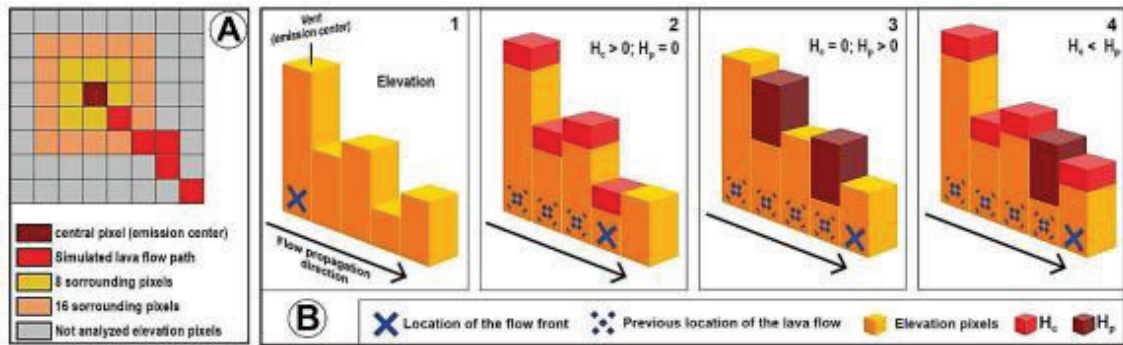


Figure 5.1: Conceptual visualization of a simulated lava in Q-LavHA. A) It starts from a source pixel to the surrounding pixels and B) the lava flow advances taking into account the thickness correction factors when filling the lower level pixels (modified by Mossoux et al., 2016).

The output file generated by Q-LavHA expresses the probability that the pixels are flooded by lava, thus generating a raster file ".asc" with a flood map that can be added to a QGIS project. This probability integrates all the flow lines calculated from one or several emission centers. The number of lines is defined by the number of iterations we have set in Q-LavHA. Apart from the raster layer, a ".txt" file is generated which gives us information on the parameters used in the simulation and the results, as well as the Fitness Index (FI) calculations. This index allows us to calculate the accuracy of the simulated lava flow, comparing it with a real mapped lava. The overlap between them is expressed as $FI_{\text{true positive}}$ values around 0 and 1. In addition, we will have two more data, the overestimation of the flow ($FI_{\text{false positive}}$) and the underestimation of the flow ($FI_{\text{false negative}}$).

6.- Analysis of the El Lentiscal eruption simulation.

Explaining the code-level operation of Q-LavHA and the three models it implements (Maximum length, Decreasing probability and FLOWGO) is the philosophy behind the lava flow models. This section shows the results obtained from the simulations performed on the El Lentiscal eruption. A series of tests are performed with the Lmax model, since it is highly recommended if a certain person does not have enough knowledge about lava properties or simply wants to establish a first contact with the plugin. In addition, the interpretation of the results is presented through studies on the performance of the input data, the limitations of the models and the importance of DEMs.

6.1.- Importance of the parameters used.

When entering the respective parameters in Q-LavHA, it is necessary to be aware of the variability that the results may have. Therefore, the resulting lava flows can be highly variable and be very different from the fit to a real lava. Although less significantly, by using the same values different simulations may take a different path.

The most important parameters for our study are those that constrain lava propagation. These are H_c and H_p correction values explained above. The simulation starts on a point center (Monte Lentiscal), from whose mapped lava we have obtained a minimum thickness of 4m (H_c) and an average thickness of 13m (H_p). The simulation was performed on a surface with an average slope of 3°. Then, the "H16" and "Probability to the square" options have been disabled in the first place since we are only interested in studying the behavior of the simulated lava flow with different thickness values. The result obtained can be seen in Figure 6.1. In this figure we can see that we have 4 different simulations, since we have varied the values of the minimum and average thickness from null values (figure 6.1A) ($H_c=0m$; $H_p=0m$) to the values of the mapped lava (figure 6.1D) ($H_c=4m$; $H_p=14m$), going through a combination of one of these two values (figure 6.1B ($H_c=4m$; $H_p=0m$) and figure 6.1C ($H_c=0m$; $H_p=14m$).

In figure 6.1A, since no specific values of minimum and average thickness have been established, the simulation does not allow the flow lines to advance correctly, due to the fact that the lava front limits their movement. Furthermore, in this case if the flow encounters a large depression the simulation of the lava flow lines stops. Therefore, a series of high probability values (redder zones) are obtained, flooding pixels with a small height difference found in the center of the channel. Using only the average thickness (Figure 6.1 B) we obtain a simulation similar to the first one of larger size, this value being theoretically more useful if combined with the minimum thickness. The value of the average thickness being larger than the value of the minimum thickness, has a greater implication in the simulation processes as presented in Figure 1.6 D. The main difference observed is the extent of the simulated lava flow, being the largest in Figure 6.1 B, this implies a better mobility over the DEM flooding from the deepest areas to the flatter areas. Finally, it is seen how the straight line from the emitting source and the lava front is shorter in Figures 6.1 C and D, being the opposite case of not applying any value for thickness, which makes it extend beyond the established distance.

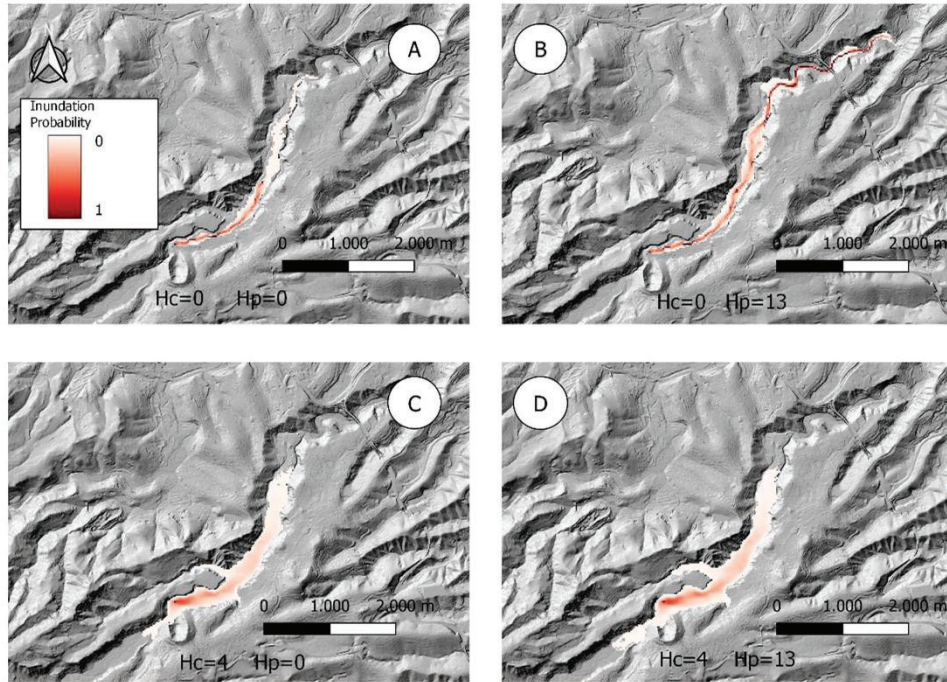


Figure 6.1: Results of lava simulations varying with the values of minimum and average thickness. The "Probability to the Square" and "H₁₆" options are disabled.

However, when we activate the options "H₁₆" and "Probability to the square" we will obtain more optimized results. A simulation more adjusted to the mapped lava (Figure 6.2). On one hand, the lava channeling effect is accentuated in the flatter areas. This is because the probability of flooding is concentrated in the center of the channel for all cases (Figure 6.2 A-D) and, at the same time, the flow width is larger especially in Figure 6.2 C and D. This is as expected because for mass conservation, the volume of lava that has not flooded allows the front to advance more, coinciding with the actual mapped lava. However, by introducing null values or only Hp (average thickness) it advances more with respect to those obtained (Figure 6.2 B).

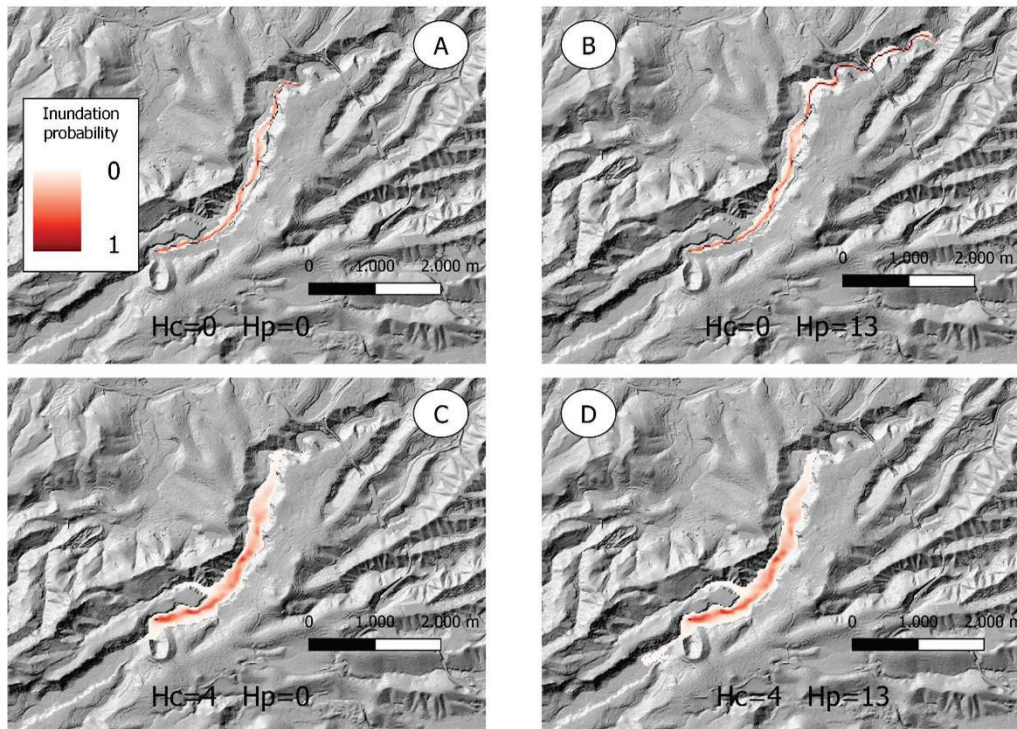


Figure 6.2: Results of lava flow simulations varying the values of minimum and average thickness.

"Probability to the Square" and "H16" options are enabled

Once these two lava flow simulation tests have been carried out, another check is made in order to find the value of H_c (minimum thickness), leaving H_p (average thickness) with a null value. With this test the behavior of the lava flow is also better understood. Figure 6.3 A presents the results of collecting FI data by performing 20 simulations obtaining a plot of FI versus H_c . The optimum value is between values 3 and 4 thickness, although for the final results we will use the value of 4 meters obtaining an overlap IF of 0.761. To the right of the graph is the simulation corresponding to the optimum value of H_c , where the maximum probability of flooding coincides to a large extent with the real lava.

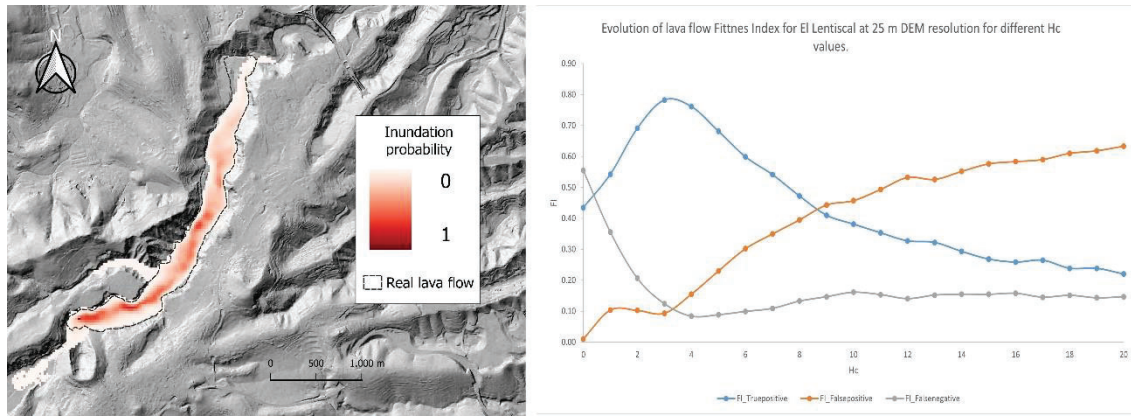


Figure 6.3: Optimal simulations with a graph representing H_c versus FI indicating the processing performed for the L_{max} model.

6.2.- Constraints on lava length and their implication for simulation models.

Which of the models used in our study should be chosen for the development of a volcanic terrain model with the lowest possible uncertainty? The key to this question will be found in the degree of coincidence or the FI index. Then, the results should match as much as possible with the actual mapping of Monte Lentiscal.

Figure 6.4 presents the result of using each of the models that have been selected for this work. Several zones can be distinguished on the simulations: one zone that matches the actual lava (light blue color), three overestimated zones (red color) and two underestimated zones (green color). In the case of figure 6.4 B made with the Decreasing Probability model, a large extension of overestimated flow lines can be observed, that is, simulated flow lines generated by the algorithm that do not coincide with the extension of the real lava. On the other hand, between Figures 6.4 A and C there are no major differences. However, analytically (Table 6.1) the FLOWGO model generates a higher percentage of overlap than the L_{max} model.

The L_{max} simulation model is one of the easiest to implement. This is due to the need to only add a single parameter (lava length) whose determination is done directly in the field by taking measurements on real lava, as well as taking the minimum and average thickness measurements of the lava flow. In contrast, the Decreasing Probability simulation model has a very low percentage of overlap (37.92%). For this model, the mean data and the standard deviation of all Holocene lavas of Gran Canaria are introduced (Appendix III). It is also necessary to input the lava length, which in turn gives us an overestimated flow extent of 60.9%. This means that most of the flow

simulated under this model is outside the actual margins of the actual lava. Finally, FLOWGO is the most data-intensive model. For this model, thermal, rheological and dynamic data must be introduced, which allow us to have a simulation much closer to the real lava, as shown in Table 6.1. However, the physicochemical data of the lava flow are determined once the material is ejected in the form of an eruption, making the computational processes slower. Therefore, the Lmax model in terms of efficiency is the most suitable model to implement.

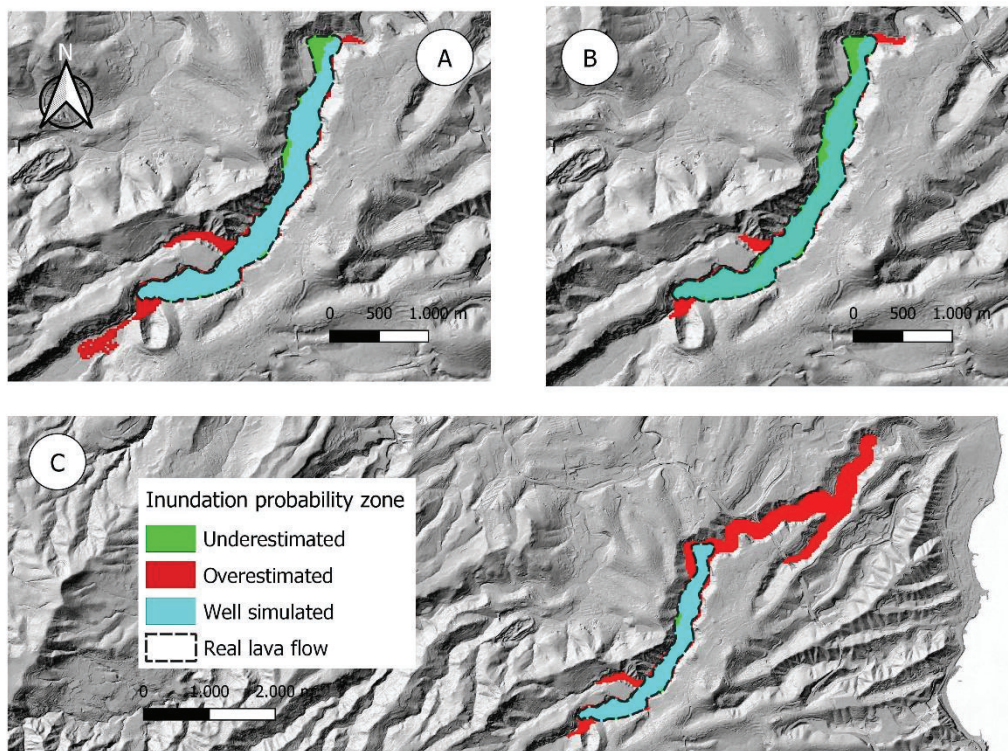


Figure 6.4: Schematized visualization of the IF values where the superposition of the real lava on the simulated one with the models A) Lmax, B) Decreasing Probability and C) FLOWGO is observed.

Table 6.1: IF values in percent indicating overlapping fraction of pixels.

Models	Well simulated pixels (%)	Underestimate d pixels (%)	Overestimated pixels (%)
L_{max}	69.75	7.85	22.39
Decreasing probability	37.92	1.17	60.9
FLOWGO	76.12	12.21	11.66

With the Lmax model the actual lava length must be corrected. This can be seen in Figure 6.5. Introducing the real mapped lava length (figure 6.5 A), it is observed that the

flow lines do not fill the real margins of the real lava, while applying the correction factor (figure 6.5 B) the simulated flow fills much of the perimeter of the real lava, even exceeding it by a few pixels at the lava front. Conservation of the IF is one of the fundamental aspects for the study. This leaves us with an underestimated fraction of 0.3553 in Figure 6.5 A, leaving a large amount of pixels without flooding (FI_{True Positive}), while in Figure 6.5 B we obtain an underestimated area of 0.785 increasing the overlap of the simulated flow.

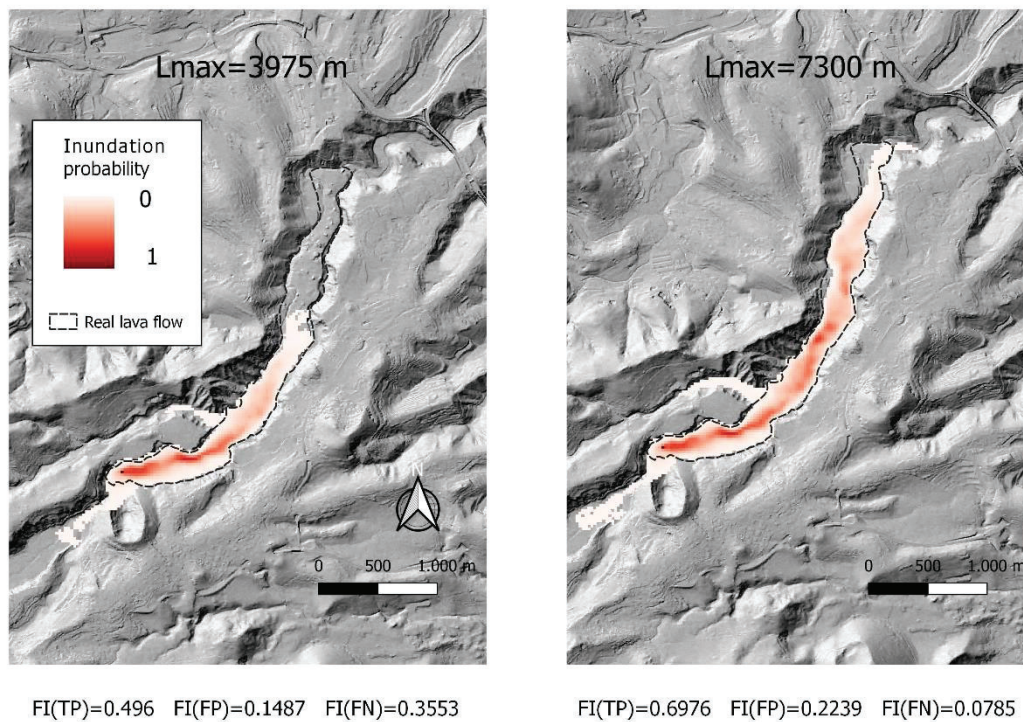


Figure 6.5: Differences in lava simulations applying different values of L_{max} ; A) without applying the correction factor, B) applying the correction factor of 1.84.

This whole occurrence is because each flow line follows an irregular path whose length is longer than the shortest length along the main channel (Mossoux et al., 2016). These types of observations are similar to those in simulations with smoother slopes. Therefore, we can assume that there is a linear relationship between the slope intensity and the correction factor used for the flow length.

6.3.- DEM characteristics and their implications for simulations

When analyzing the propagation of a lava flow in the same topography visualized in DEMs with different resolutions, the behavior of the lava flow to flood pixels may vary. DEMs are the main basis for simulations and therefore their resolution and morphology significantly influence the results.

The first implications of the resolution of a DEM is its implication on the main parameters such as lava flow thickness. According to Mossoux et al. (2016), it has been shown that the optimal value of H_p depends on the resolution of the DEM to be used, varying in turn with it. However, the calculated values of H_p always tend to the real lava. Therefore, the value of H_p is of great importance, especially in high resolution DEMs.

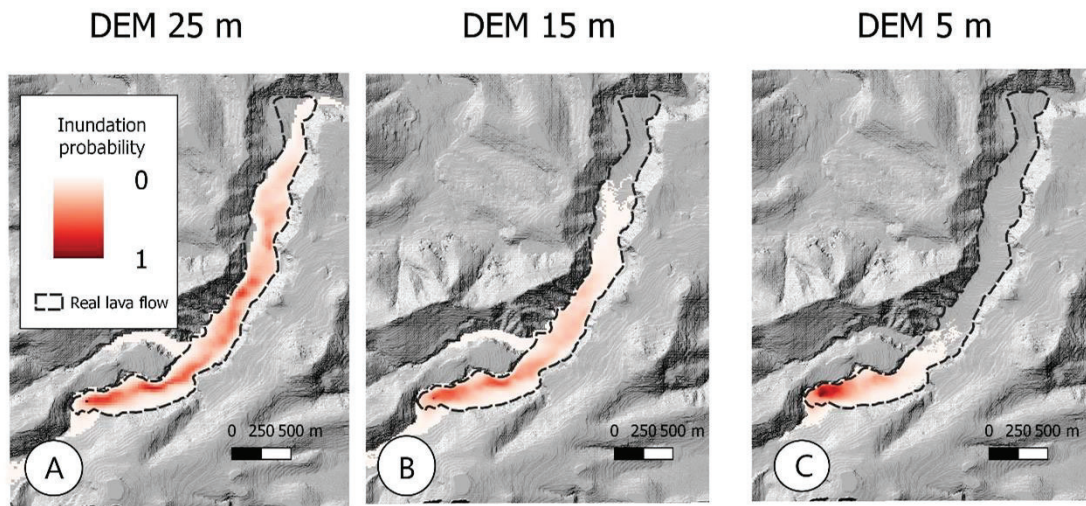


Figure 6.6: Probability of lava flow flooding using DEMs with different resolutions.

The analysis of the simulations in the same DEM but with different resolution is shown in Figure 6.6, for which we have used the L_{max} model. Figure 6.6C has the smallest pixel size (5X5 meters), which allows us to observe in more detail the geometry of the lava flow. This simulation most likely floods the gully channel, having adequate overlap during the first few meters of the gully until the simulation stops abruptly. The flow lines stop extending even leaving 62.18% of the actual lava covered, having 31.47% overlap (table 6.2). The simulated flows in the 25 and 15 m resolution DEMs (Figure 6.6A and B) lose detail of the topography but gain in the fit index up to 69.76% in Figure 6.6 A. Therefore, as we increase the DEM resolution the simulated flow length decreases. In addition, it should be emphasized that the processing times are highly variable, being higher the smaller the pixel size.

Table 6.2: IF values from different DEMs resolution.

DEM resolution	$FI_{true\ positive}$	$FI_{false\ positive}$	$FI_{false\ negative}$
5 m	0.3147	0.0635	0.6218
15 m	0.5808	0.1899	0.2293

25 m	0.6976	0.2239	0.0785
------	--------	--------	--------

The last aspect to be studied is the behavior of the lava flow in the morphology, this is because the most affected flood zones are those with positive slopes (downward) and flat areas. El Lentiscal presented a different morphology from the present one. It is possible to visualize how the paleo-relief of the gully is U-shaped and with a single axis, through which the lava from the eruption flowed, coinciding in 69.76% with the simulated lava, using the Lmax model, as shown in Figure 6.7A. The relief resulting from the eruption leaves us with an inverted structure in the center of the gully channel. Over time, the lava becomes a divide leaving two axes of the Guinguada gully through which the water flows during the rainy season. In the case of figure 6.7B, a simulation is made on the current topography being an eruption subsequent to the one studied. The lava from this supposed eruption would partially cover the existing lava flow, with a greater probability of flooding the ravine on the eastern flank of the lava. In this case the simulation overlap is 54.85% being very adequate, however, the probability of flooding varies at low probability values.

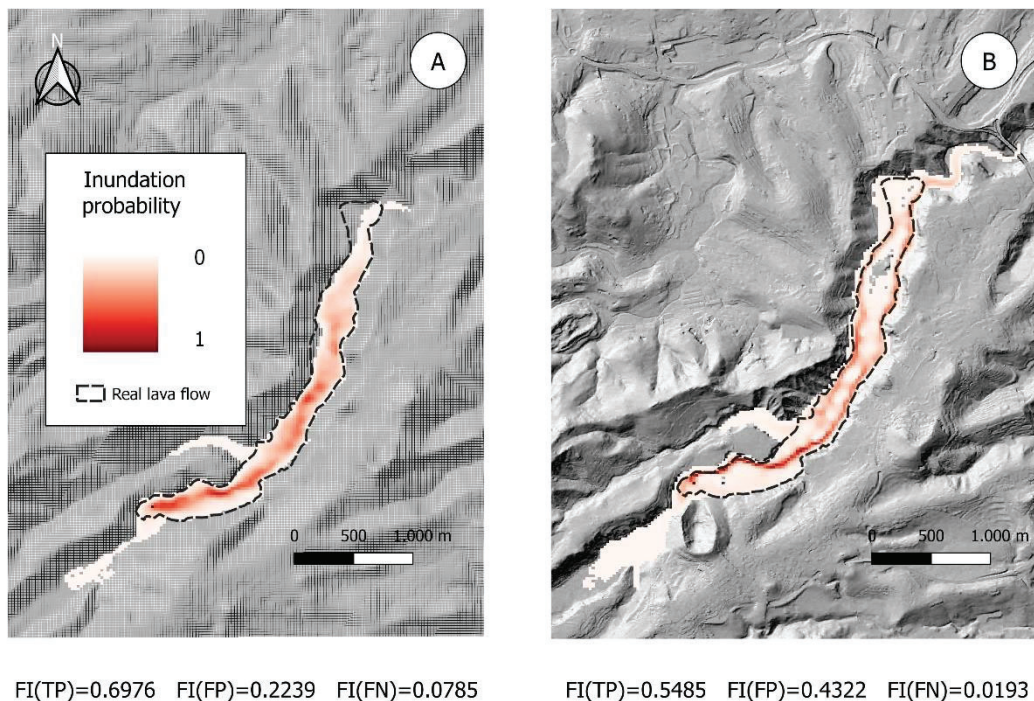


Figure 6.7: Probability of lava flow flooding using DEMs with different topographies.

7.- Conclusion

Throughout the study, the importance of GIS in volcanological studies and in the prevention in case of volcanic crisis has been emphasized. In the case of this paper, the volcanological history of the island of Gran Canaria has been considered from the Miocene (approximately 14.5 Ma) to the present (Holocene). The methodology implemented has allowed us to carry out subsequent evaluations and to create management programs in case of future eruptions in the islands. We have worked using digital maps from which we have obtained cartographic data of the El Lentiscal eruption (volcanic cone, pyroclastic mantle, horizontal dispersion and lava flow). With all the geographic data obtained throughout the work and the contour lines we reconstructed the area affected by our studied eruption to obtain the pre-eruptive topography. Once this topography is obtained, it can be understood that the volcanic edifice grew on a gently sloping hillside and the lava flow flooded the bottom of the existing paleo ravine during that period of time. With the passage of time, this gully opened its way dismantling part of the volcanic cone and the E flank of the lava flow, this is due to the nature of these materials. Thus, the Guinguada ravine opened its way, characterized by gentle slopes and in this section having a "V" shape as shown in Figure 7.1.



Figure 7.1: Field photo in the Guinguada ravine.

Also, for this study we have compared the real lava with simulations performed with the Q-LavHA plugin comparing the three simulation models that it incorporates (Lmax, Decreasing Probability and FLOWGO). Morphometric data of the lava flow have been used for all models. In addition, a series of tests have been carried out to check how variations in the minimum and average thickness values affect the simulation of the lava flow, as well as the implication in the simulation of the length of the lava flow and the resolution of the DEM used. Among the three simulation models used in the work the

one that has not obtained good results is the Decreasing Probability model giving very low FI values. On the contrary, the Lmax and FLOWGO models are the most suitable models to implement, being the first one the most efficient in terms of computational process speed and the second one the most efficient in analytical terms.

Thanks to the data obtained in this study, using the appropriate and optimized models and knowing the characteristics of lava from Mount Lentiscal, it is possible to generate realistic emergency plans for a possible eruption of the same characteristics, since these simulations have determined that lava would flow as it did at the time of the eruption. All this information allows minimizing human and material losses in the affected areas. In addition, one of the advantages of using this type of methodology is to avoid unnecessary use of security systems in low-risk areas.

8.- Discussion

As mentioned in the introduction of this paper, volcanic eruptions are a fact that humans as inhabitants of planet Earth have to live with. For this, GIS gives us the facility to know how a lava flow would behave from digitized maps and sophisticated plugins.

With the last eruption and thanks to the work of PEVOLCA (Canary Islands Volcanic Emergency Plan) that brought together several public institutions such as the IGN (National Geographic Institute) and the IGME (Spanish Geological and Mining Institute) and the use of GIS, was able to generate an emergency plan to avoid human losses. The help provided by the council of La Palma and the participation of the University of La Laguna (Tenerife) in the creation of said emergency plan should also be highlighted. Thanks to the GIS, it was possible to know in advance where the lava would flow and even where it would end up in the sea, generating maps as we can see in figure 8.1.

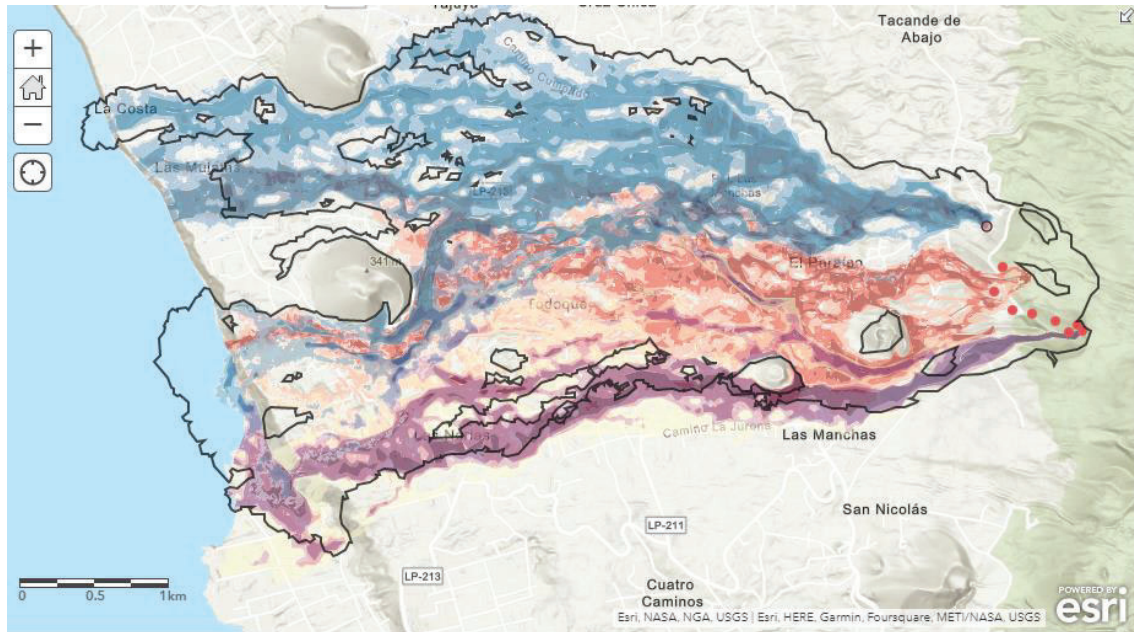


Figure 8.1: Four simulations are shown overlaid at different times of the eruption (*Riesgo volcánico*, 2021).

Appendix

Appendix I: Standard and specific parameters used in the FLOWGO model for the El Lentiscal eruption and their analytical results from the optimal simulation.

Parameters	El Lentiscal	
Location UTM (X,Y)	(453.296, 3.103.698)	
Resolution DEM (m)	25	
H _c (m)	4	
H _p (m)	13	
FI _{true positive}	0.7612	
FI _{false positive}	0.1166	
FI _{false negative}	0.1222	

Parameters	El Lentiscal	Source
Lava velocity		
Emission rate (m ³ /s)	100	<i>Estimated from various authors</i>
Viscosity (Pa*s)	3,57	<i>Calculated</i> $\mu(\theta) = \mu_i(1 - R\theta)^{-2,5}$
Initial phenocrystal mass fraction	0,15	<i>Petrographically estimated</i>
Lava channel ratio (width/thickness)	19,8	<i>Calculated from</i> <i>Rodriguez-González (2009)</i>
Thermal parameters lava		
T (eruption temperature) (°C)	1250	<i>Typical of very basic lavas</i>
T (temperatura outer layer lava) (°C)	600	<i>Harris y Rowland (2001),</i> <i>Harris et al. (2015)</i>
Difference (Indoor lava and outdoor temp.) (°C)	150	<i>Harris y Rowland (2001),</i> <i>Harris et al. (2015)</i>
d (constant)	-0,16	<i>Mossoux et al. (2016)</i>
Viscosity and elasticity		
a (constant) (1/K)	0,04	<i>Dragoni (1989)</i>
b (constant) (Pa)	0,01	<i>Dragoni (1989)</i>
c (constant) (1/K)	0,08	<i>Dragoni (1989)</i>
Constant speed		
Gravity (m/s ²)	9,81	-
Conventional parameters		
Wind speed (m/s)	5	<i>Harris y Rowland (2001)</i>
Ch (friction wind speed)	0,0036	<i>Harris y Rowland (2001)</i>
Air temperature (°C)	25	<i>Estimada</i>
Air density (kg/m ³)	0,4412	<i>Harris y Rowland (2001)</i>
Specific heat capacity of air (J/kg.K)	1099	<i>Harris y Rowland (2001)</i>
Density and vesicularity of lava		
Density DRE (dense rock equivalent) (kg/m ³)	2880	<i>Calculated</i> $\rho = (1 - \theta b)\rho_{DRE}$
Vesicularity (%)	0,03	<i>Petrographically estimated</i>
Crystallisation parameters		
Tasa de crecimiento	0,004	<i>Estimated from various authors</i>
L (latent heat of crystallisation) (J/kg)	350000	<i>Harris y Rowland (2001)</i>
R (Inv. Of maximum cristal concentration)	1,51	-

<i>Driving parameters</i>		
Thickness of outer lava layer (%)	10	<i>Various authors</i>
T (Temp. At base outer layer lava) (°C)	600	<i>Various authors</i>
Thermal conductivity of lava(W/m.K)	2,05	<i>Cordonnier et al. (2014) y Mossoux et al. (2016)</i>
<i>Radiation parameters</i>		
Sbc (cons. of Stephan-Boltzmann (W/m ² .K ⁴))	5,67E-08	-
e (emissivity of basalt)	0,95	<i>Harris y Rowland (2001); Cordonnier et al. (2014)</i>

Appendix II: Standard parameters used in the Lmax model for the El Lentiscal eruption and their analytical results from an optimal simulation.

Parameters	El Lentiscal
Location UTM (X,Y)	(453.296, 3.103.698)
Resolution DEM (m)	25
Lenght (m) - L_{max}	$3.975^{(a)} * 1,84 = 7.300$
H _c (m)	4
H _p (m)	13
FI _{true positive}	0.6976
FI _{false positive}	0.2239
FI _{false negative}	0.0785

Appendix III: Standard parameters used in the Decreasing Probability model for the El Lentiscal eruption and their analytical results from an optimal simulation.

Parameters	El Lentiscal
Location UTM (X,Y)	(453.296, 3.103.698)
Resolution DEM (m)	25
Mean _{Holoceno} (m)	3.793
SD _{Holoceno} (m)	2.702
H _c (m)	4
H _p (m)	13
FI _{true positive}	0.3857
FI _{false positive}	0.6008
FI _{false negative}	0.0136

Bibliography

Antenucci, J., Brown, K., Croswell, P., Kevany, M., & Archer, H. (1991). *Geographic Information Systems*. <https://link.springer.com/book/9781461367550>

Clarke, K. C. (1986). Advances in Geographic Information Systems. *Computers, Environment and Urban Systems*, 10(3), 175-184. [https://doi.org/10.1016/0198-9715\(86\)90006-2](https://doi.org/10.1016/0198-9715(86)90006-2)

de' Michieli Vitturi, M., & Tarquini, S. (2018). MrLavaLoba: A new probabilistic model for the simulation of lava flows as a settling process. *Journal of Volcanology and Geothermal Research*, 349, 323-334. <https://doi.org/10.1016/j.jvolgeores.2017.11.016>

Dueker, K. J. (1979). Land resource information systems: A review of fifteen years experience. *Geo-Processing (Netherlands)*.

[https://scholar.google.com/scholar_lookup?title=Land+resource+information+systems
%3A+a+review+of+fifteen+years+experience&author=Dueker%2C+K.J.+%28Portland+S
tate+Univ.%2C+Oregon+%28USA%29.+School+of+Urban+Affairs%29&publication_year
=1979](https://scholar.google.com/scholar_lookup?title=Land+resource+information+systems+%3A+a+review+of+fifteen+years+experience&author=Dueker%2C+K.J.+%28Portland+State+Univ.%2C+Oregon+%28USA%29.+School+of+Urban+Affairs%29&publication_year=1979)

Goodchild, M. F. (1985). Geographic information systems in undergraduate geography: A contemporary dilemma. *Operational Geographer*, 8, 34-38.

Google Earth. (2022).

[https://earth.google.com/web/search/Monte+Lentiscal/@28.05702397,-
15.47458203,333.5101699a,1990.47369094d,35y,-
0.09792882h,44.28008753t,0r/data=CnkaTxJJCiQweGM0MDk2OTUwNmZIM2VIMTowe
eDZjZGFjZWU3ZTQyNmQwMzYZbBZ5o6ALPEAhRgsrcA3zLsAqD01vbnRIIExlbnRpc2Nh
bgBgBIAEiJgokCfSpkSIEakLAEQVIPV__ckLAGbCEQdE022VAIcULOF1e1WVA](https://earth.google.com/web/search/Monte+Lentiscal/@28.05702397,-15.47458203,333.5101699a,1990.47369094d,35y,-0.09792882h,44.28008753t,0r/data=CnkaTxJJCiQweGM0MDk2OTUwNmZIM2VIMToweDZjZGFjZWU3ZTQyNmQwMzYZbBZ5o6ALPEAhRgsrcA3zLsAqD01vbnRIIExlbnRpc2NhbgBgBIAEiJgokCfSpkSIEakLAEQVIPV__ckLAGbCEQdE022VAIcULOF1e1WVA)

Harris, A. J., & Rowland, S. (2001). FLOWGO: A kinematic thermo-rheological model for lava flowing in a channel. *Bulletin of Volcanology*, 63(1), 20-44.

<https://doi.org/10.1007/s004450000120>

Masser, I. (2014). *Governments And Geographic Information*. CRC Press.

<https://doi.org/10.1201/9781482267891>

- Mossoux, S., Saey, M., Bartolini, S., Poppe, S., Canters, F., & Kervyn, M. (2016). Q-LAVHA: A flexible GIS plugin to simulate lava flows. *Computers & Geosciences*, *97*, 98-109.
<https://doi.org/10.1016/j.cageo.2016.09.003>
- Raveneau, J. (1988). Burrough, P.A. (1986) Principles of Geographical Information Systems for Land Resources Assessment. Oxford, Oxford University Press, 193 p. *Cahiers de géographie du Québec*, *32*(85), 76-77. <https://doi.org/10.7202/021932ar>
- Richardson, P., & Karlstrom, L. (2019). The multi-scale influence of topography on lava flow morphology. *Bulletin of Volcanology*, *81*(4), 21. <https://doi.org/10.1007/s00445-019-1278-9>
- Rielo, A. F. (2002). *Modelización física y simulación numérica de procesos eruptivos para la generación de mapas de peligrosidad volcánica* [Http://purl.org/dc/dcmitype/Text, Universidad Complutense de Madrid].
<https://dialnet.unirioja.es/servlet/tesis?codigo=197535>
- Riesgo volcánico*. (2021). <https://volcan.lapalma.es/apps/simulaci%C3%B3n-ull>
- Rodríguez González, A. (2009). *El vulcanismo holoceno de Gran Canaria: Aplicación de un sistema de información geográfico*.
<https://accedacris.ulpgc.es/jspui/handle/10553/1894>
- Rodriguez-Gonzalez, A., Fernandez-Turiel, J. L., Perez-Torrado, F. J., Gimeno, D., & Aulinas, M. (2010). Geomorphological reconstruction and morphometric modelling applied to past volcanism. *International Journal of Earth Sciences*, *99*(3), 645-660.
<https://doi.org/10.1007/s00531-008-0413-1>
- Rodriguez-Gonzalez, A., Perez-Torrado, F. J., Fernandez-Turiel, J. L., Aulinas, M., Paris, R., & Moreno-Medina, C. (2018). The Holocene volcanism of Gran Canaria (Canary Islands, Spain). *Journal of Maps*, *14*(2), 620-629.
<https://doi.org/10.1080/17445647.2018.1526717>

SMITH, T. R., MENON, S., STAR, J. L., & ESTES, J. E. (1987). Requirements and principles for the implementation and construction of large-scale geographic information systems.

International Journal of Geographical Information Systems, 1(1), 13-31.

<https://doi.org/10.1080/02693798708927790>

Memoria final del Trabajo Fin de Grado

Introducción

Mi elección de prácticas fue un poco complicada, debido a que desde tercero no tenía muy claro en qué grupo quería meterme para hacer las prácticas extracurriculares. Sin embargo, una vez que curse en el primer semestre de cuarto curso del grado la asignatura de Técnicas de la Información Geográfica en el Ámbito Geológico (TIG), donde se muestra los usos básicos de los Sistemas de Información Geográfica (SIG). A partir de entonces hable con el tutor de la asignatura, el profesor Alejandro Rodríguez González. Le pedí información sobre las prácticas del grupo GEOVOL.

La información que me dio el profesor Alejandro Rodríguez fue muy buena y, la verdad, me gustó mucho la filosofía del grupo.

El grupo pertenece al Instituto Universitario de Estudios Ambientales y Recursos Naturales (IUNAT), se ubica en la facultad de ciencias básicas y trabaja en la rama de la geología, más objetivamente en vulcanología. Para realizar las prácticas he tenido el laboratorio B-204 del departamento de biología de la facultad de ciencias básicas, así también tenía disponible un ordenador para poder realizar todas las actividades.



Figura 1: Logo del grupo GEOVOL de la ULPGC.

Las expectativas que tenía antes de empezar las prácticas eran muy buenas, debido a que sabía como trabajaba mi tutor, el profesor Alejandro Rodríguez, y la información que me habían facilitado era muy buena. Una vez finalizado y visto el resultado de todas

las actividades mis expectativas han sido superadas, por el trato que he recibido, las ayudas que he recibido y la formación que se me ha facilitado.

Desarrollo de las prácticas

El principio de las prácticas Alejandro Rodríguez González me enseñó el taller del grupo en el garaje de la facultad de ciencias básicas, donde realizan las muestras para hacer las laminas delgadas para poder mirar al microscopio petrográfico y obtener la geoquímica de las muestras tomadas en el campo.

También, se me facilitó una bibliografía bastante amplia para entender la filosofía SIG y entender mejor el programa que se iba a utilizar en el transcurso de las prácticas. Dicho programa es el Q-GIS (Figura 2), un software libre que se utiliza para todas las actividades que engloba los SIG.



Figura 2: Logo de la versión 3.16 de Q-GIS.

Para un mejor manejo del programa hemos realizado varias clases de formación en distintas partes de las prácticas. La primera clase me enseñaron las nociones básicas del programa y descargas de herramientas necesarias para el desarrollo de la práctica, concretamente las herramientas que tuve que descargar fueron Q-LavHa (para la parte de simulación de flujos de lava) y otra herramienta con el nombre de terrain profile (para realizar perfiles topográficos). En esta clase también se enseñó a realizar mis propias figuras controlando las coordenadas de los mapas, poner el norte, poner la escala y poner un mapa de localización.

También se me explicó el proceso que se sigue cuando tienen que preparar una muestra para el análisis geoquímico y hacer las láminas finas para poder ver la muestra al microscopio petrográfico. Dicho proceso es el siguiente:

- 1.- En el campo se toma una muestra con martillo de geólogo con apariencia de roca fresca, es decir, una roca donde los minerales que la componen no estén tan alterados (Figura 3).



Figura 3: Muestra de roca de la colada de lava de la erupción del Lentiscal.

2.- Una vez en el taller, se limpian las paredes de la muestra con una sierra especial y refrigerada con agua, y se cortan varios tacos de unos 5X5 cm para mandarlos a la Universidad de Barcelona para elaborar las láminas delgadas (Figura 4).



Figura 4: A) Sierra para cortar la muestra en tacos operativa en el taller de geología. B) Ejemplo de tacos cortados por la sierra de la muestra anteriormente mencionada.

3.- Después de cortar la muestra en tacos se usa una machacadora, con los tacos sobrantes, introduciéndolos uno a uno para obtener un tamaño de grano de gravas (Figura 5).



Figura 5: A) Machacadora operativa en el taller de geología de la facultad de Ciencias Básicas. B) Ejemplo del resultado una vez que los tacos de la muestra han sido machacados.

4.- Por último, se usa un mortero de ágata, para obtener un polvo homogéneo de la muestra, parte del cual se envía a la Universidad de Barcelona para realizar los estudios geoquímicos pertinentes (Figura 6).



Figura 6: Mortero de ágata en el taller de geología.

Sin embargo, esta parte de la práctica era simple curiosidad, debido a que la verdadera meta era entender bien los conocimientos de morfometría y a utilizar bien los software

de SIG.

Para finalizar con las prácticas se ha realizado una salida de campo donde el profesor Alejandro Rodríguez me ha enseñado a como interpretar las curvas de nivel de un mapa en el terreno de estudio, para que a la hora de realizar las simulaciones de lava se tenga una visión 3D del relieve de la zona.

Estas prácticas tuvieron una duración de tres meses, desde el 3 de febrero hasta el 13 de abril de 2021, lo que suma una duración de aproximadamente 3 meses de prácticas.

Es un grupo de investigación la cual se encuentra muy bien posicionada en el ámbito de la investigación geológica. Sin embargo, el número de integrantes de dicho grupo de investigación es muy reducido. Con respecto a la relación con el personal del grupo era casi nula, debido a que casi siempre estaba solo en el laboratorio.

Conclusión

En conclusión, estas prácticas me han resultado muy satisfactorias tanto desde el punto de vista del aprendizaje como desde el punto de vista científico. Además, el profesor Alejandro siempre estaba dispuesto a ayudarme con cualquier duda que tenía y para la corrección de las actividades realizadas en el transcurso de las prácticas.

Los puntos positivos de la realización de dichas prácticas es la preparación previa, la ayuda del tutor siempre que el mismo pueda y te prepara para una salida profesional, no solo en el ámbito de la investigación sino también en el ámbito de las administraciones públicas en campos como manejo del territorio o medio ambiente, esto se debe a que la utilidad de los SIG abarca muchos campos y tienen muchas habilidades diferentes dependiendo del campo de trabajo.

Como puntos negativos tenemos el número de integrantes del grupo, por lo que estaba solo casi todos los días en el laboratorio, y también el laboratorio necesita una renovación de material, sobre todo en ordenadores.

El aprendizaje que he recibido durante la práctica ha sido bastante bueno y muy claro. Esto es gracias a las explicaciones del profesor Alejandro Rodríguez las cuales eran muy simples y claras para poder entenderlo desde el principio, explicando cada proceso paso a paso.

Por último, repito a modo de sugerencia que se mejoren los ordenadores del laboratorio, ya que son la herramienta principal de estas prácticas, otra sugerencia es aumentar el número de integrantes del grupo para poder tener varios puntos de vista de la aplicación de los SIG en diferentes ámbitos.

